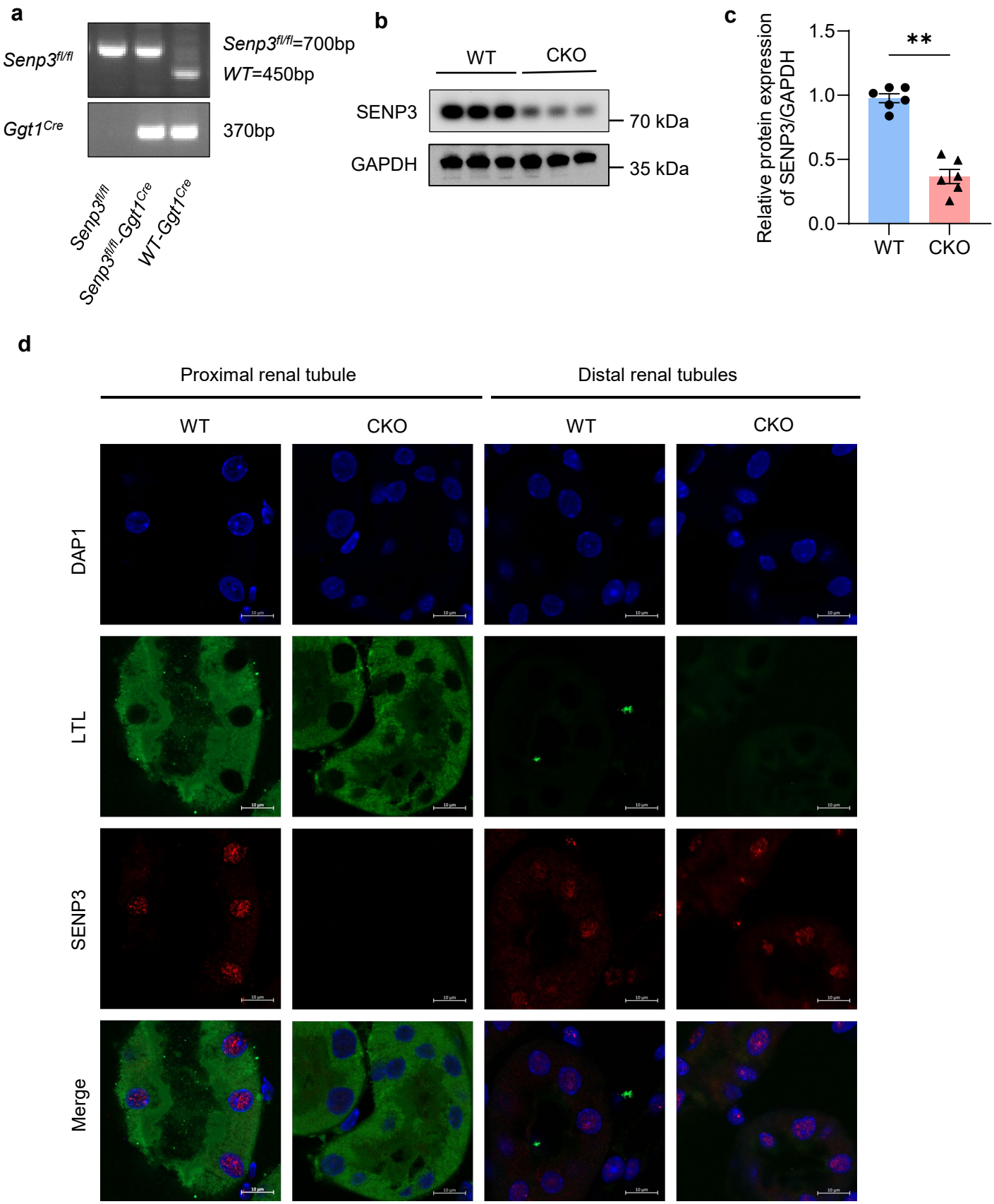

Figure S1 Successful knockout of SENP3 in renal tubular cells. (a) Genotyping of mice by PCR analysis of *Senp3* and *Ggt1* (control) in toe tissue DNA. (b-c) SENP3 protein levels were significantly reduced in renal tissues of *Senp3* conditional knockout (CKO) mice compared to WT littermates. Data: mean ± SEM (n=6); **p < 0.01. (d) Immunofluorescence staining confirmed SENP3 deficiency specifically in renal tubular cells. Scale bar: 10 μm.

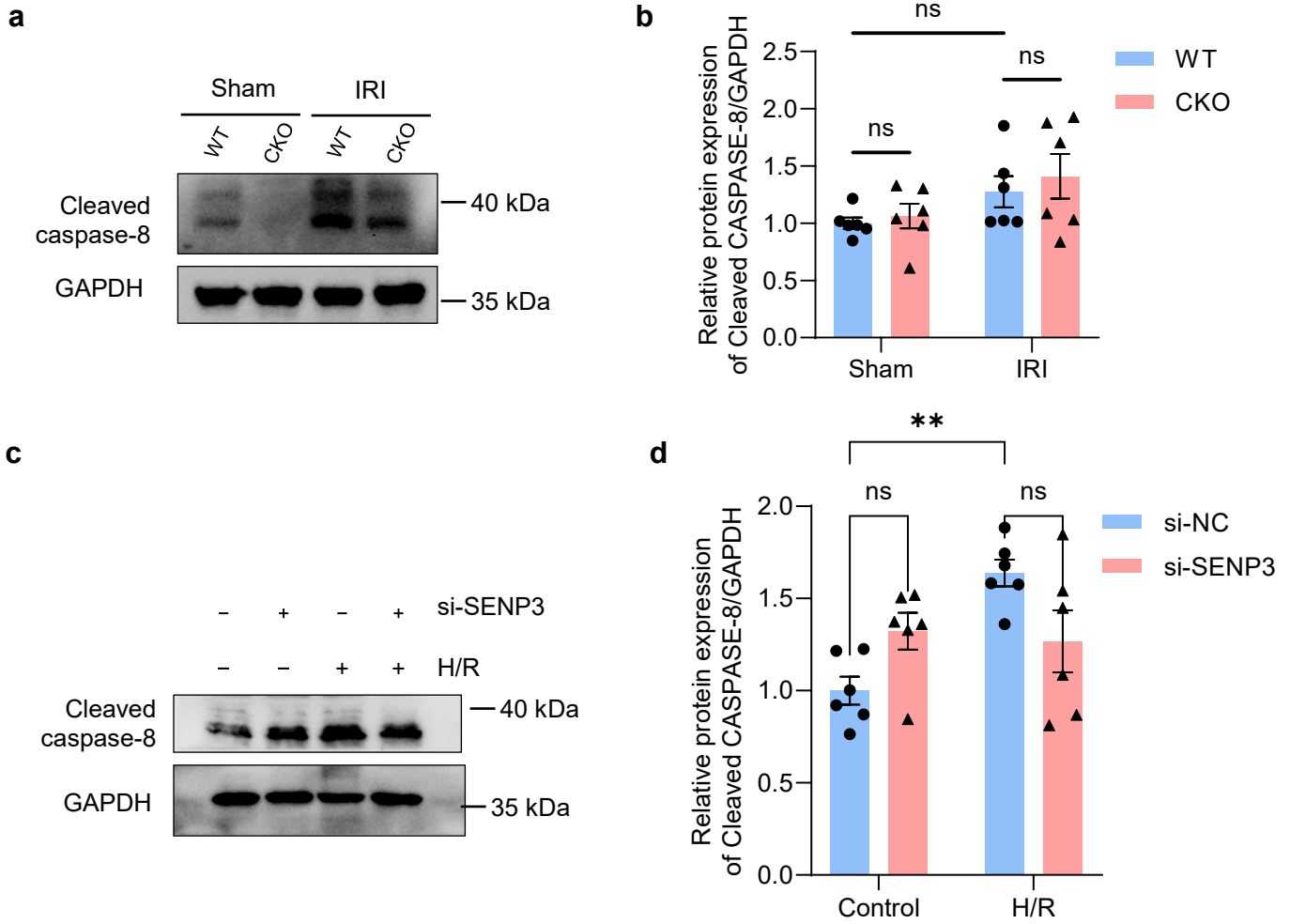

Figure S2 SENP3 deficiency does not reduce cleaved caspase-8 expression following renal IRI or H/R treatment. (a-b) Cleaved caspase-8 levels in kidney tissues of wild-type (WT) and Senp3 conditional knockout (CKO) mice after ischemia-reperfusion injury (IRI). (c-d) Cleaved caspase-8 expression in TCMK1 cells subjected to hypoxia-reoxygenation (H/R) with or without SENP3 knockdown. Data represent mean ± SEM (n=6). **p < 0.01; ns, not significant.

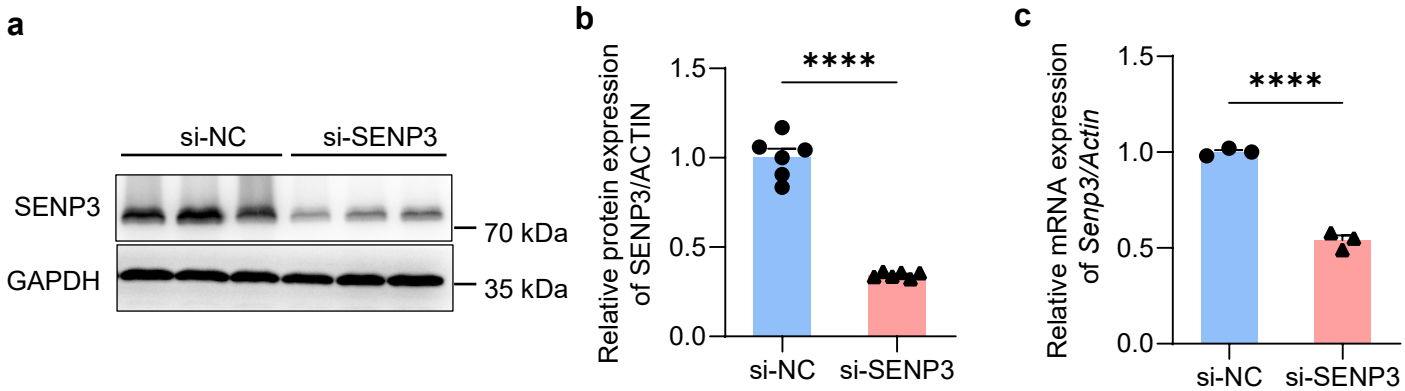

Figure S3 Efficiency of SENP3 knockdown in TCMK1 cells. (a-b) Western blot analysis and quantification showing significant reduction of SENP3 protein levels in TCMK1 cells transfected with SENP3-targeting siRNA (si-SENP3) compared to negative control siRNA (si-NC). Data represent mean ± SEM (n=6). ****p < 0.0001. (c) RT-qPCR analysis confirmed transcriptional silencing of *Senp3* in siRNA-transfected cells. Data represent mean ± SEM (n=3). ****p < 0.0001.

```
Query  1    MKETIQGTGSWGPEPPGPGIPPAYSSPRRERLRWPPPPKPRLKSGGGFGPDPGSGTTVPA  60
            MKETIQGTGSWGPEPPGPG    YS+PRRERLRWP PPKPRLKSGGGFGPDPGSGTTVP
Sbjct  1    MKETIQGTGSWGPEPPGPGT--TYSNPRRERLRWPLPPKPRLKSGGGFGPDPGSGTTVPT  58

Query  61   RRLPVPRPSFDASASEEEEEEEEEDEDEEEVAAWRLPPRWSQLGTSQRPRPSRPTHRK  120
            RRLP PRPSFDASASEEEEEEEE+    EEEVAAWRLPPRW QLG SQR R  RP+HRK
Sbjct  59   RRLPAPRPSFDASASEEEEEEEED----EEEVAAWRLPPRWGQLGASQRSRALRPSHRK  114

Query  121  TCSQRRRRAMRAFRMLLYSKSTSLTFHWKLWGRHRGRRRGLAHPKNHLSPQQGGATPQVP  180
            TCSQRRRRAMRAF+MLLYSKSTSLTFHWKLWGRHRGRRR LAHPKNHLSPQ+GGATPQVP
Sbjct  115  TCSQRRRRAMRAFQMLLYSKSTSLTFHWKLWGRHRGRRRNLAHPKNHLSPQEGGATPQVP  174

Query  181  SPCCRFDSPRGPPPPRLGLLGALMAEDGVRGSPPVPSGPPMEEDGLRWTPKSPLDPDSGL  240
            SPCCRFDSPRG PPPRLGLLGALMAEDG+RGSPPVPSGPPMEEDGLRWTPKSPLDPDSGL
Sbjct  175  SPCCRFDSPRGLPPPRLGLLGALMAEDGMRGSPPVPSGPPMEEDGLRWTPKSPLDPDSGL  234

Query  241  LSCTLPNGFGGQSGPEGERSLAPPDASILISNVCSIGDHVAQELFQGSDLGMAEEAERPG  300
            LSCTLPNGFGG SGPEGERSLAPPDASILISNVCSIGDHVAQELFQ SDLG+AEEA+R G
Sbjct  235  LSCTLPNGFGGLSGPEGERSLAPPDASILISNVCSIGDHVAQELFQSSDLGIAEEADRTG  294

Query  301  EKAGQHSPLREEHVTCVQSILDEFLQTYGSLIPLSTDEVVEKLEDIFQQEFSTPSRKGLV  360
            EKAGQHSPLREEHVTCVQSILDEFLQTYGSLIPLSTDEVVEKLEDIFQQEFSTPSRK LV
Sbjct  295  EKAGQHSPLREEHVTCVQSILDEFLQTYGSLIPLSTDEVVEKLEDIFQQEFSTPSRKSLV  354

Query  361  LQLIQSYQRMPGNAMVRGFRVAYKRHVLTMDDLGTLYGQNWLNDQVMNMYGDLVMDTVPE  420
            LQLIQSYQRMPGNAMVRGFRV+YKRHVLTMDDLGTLYGQNWLNDQVMNMYGDLVMDTVPE
Sbjct  355  LQLIQSYQRMPGNAMVRGFRVSYKRHVLTMDDLGTLYGQNWLNDQVMNMYGDLVMDTVPE  414

Query  421  KVHFFNSFFYDKLRTKGYDGVKRWTKNVDIFNKELLLIPIHLEVHWSLISVDVRRRTITY  480
            KVHFFNSFFYDKLRTKGYDGVKRWTKNVDIFNKELLLIPIHLEVHWSLISVDVRRRTITY
Sbjct  415  KVHFFNSFFYDKLRTKGYDGVKRWTKNVDIFNKELLLIPIHLEVHWSLISVDVRRRTITY  474

Query  481  FDSQRTLNRRCPKHIAKYLQAEAVKKDRLDFHQGWKGYFKMNVARQNNDSDCGAFVLQYC  540
            FDSQRTLNRRCPKHIAKYLQAEAVKKDRLDFHQGWKGYFKMNVARQNNDSDCGAFVLQYC
Sbjct  475  FDSQRTLNRRCPKHIAKYLQAEAVKKDRLDFHQGWKGYFKMNVARQNNDSDCGAFVLQYC  534
                                                          *

Query  541  KHLALSQPFSFTQQDMPKLRRQIYKELCHCKLTV  574
            KHLALSQPFSFTQQDMPKLRRQIYKELCHCKLTV
Sbjct  535  KHLALSQPFSFTQQDMPKLRRQIYKELCHCKLTV  568
```

Figure S4 Sequence alignment of human and mouse SENP3 catalytic domains.
BLAST analysis reveals conserved cysteine residues in the catalytic domains of human (top) and mouse (bottom) SENP3. The critical catalytic cysteine is positioned at C532 in human SENP3 and C526 in mouse SENP3 (indicated by red boxes).

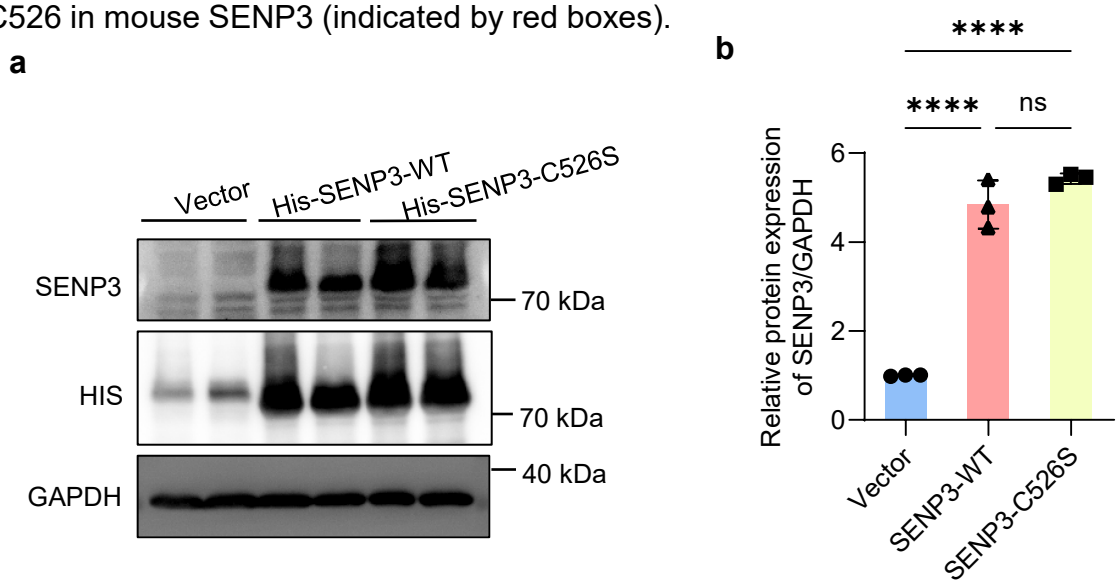

Figure S5 Lentiviral overexpression of His-tagged SENP3 variants in TCMK1 cells. (a-b) Western blot analysis and quantification demonstrating successful expression of His-tagged wild-type SENP3 (SENP3-WT) and catalytically inactive mutant (SENP3-C526S) in TCMK1 cells compared to empty vector control. The C526S mutation (catalytic domain null) did not affect protein expression levels. Data represent mean ± SEM (n=6). ns, not significant; ****p < 0.0001.

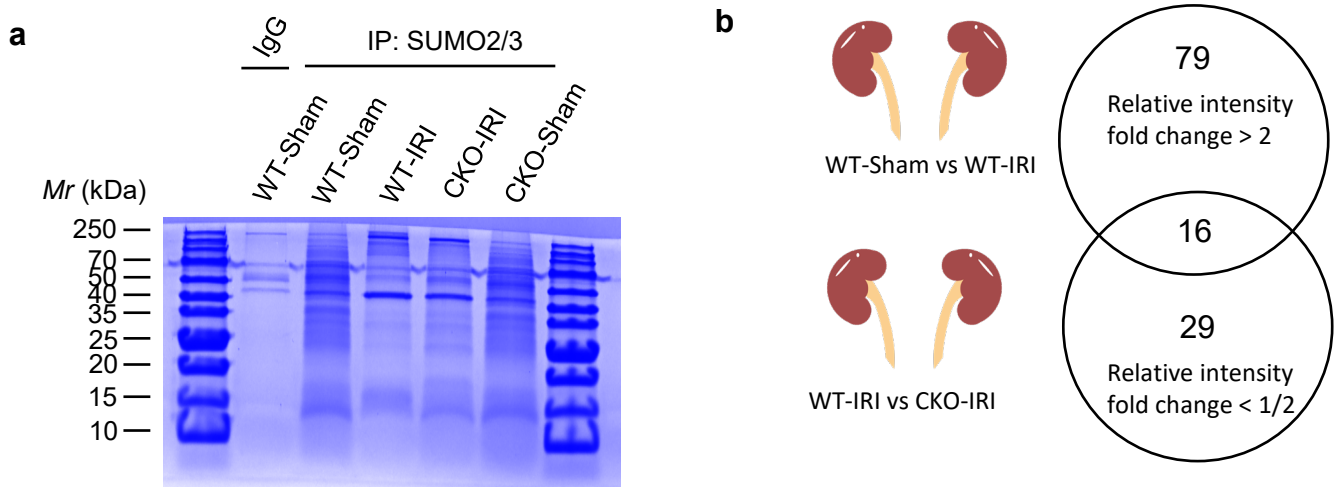

Figure S6 Identification of SUMO2/3-modified proteins in renal IRI. (a) Coomassie blue staining of SUMO2/3-conjugated proteins immunoprecipitated from kidney tissues of wild-type (WT) and *Senp3* conditional knockout (CKO) mice following ischemia-reperfusion injury (IRI). (b) Schematic workflow for liquid chromatography-mass spectrometry (LC-MS) analysis and bioinformatic screening of SUMO2/3 target proteins. Differential bands (indicated by arrows in panel a) were excised for proteomic identification.

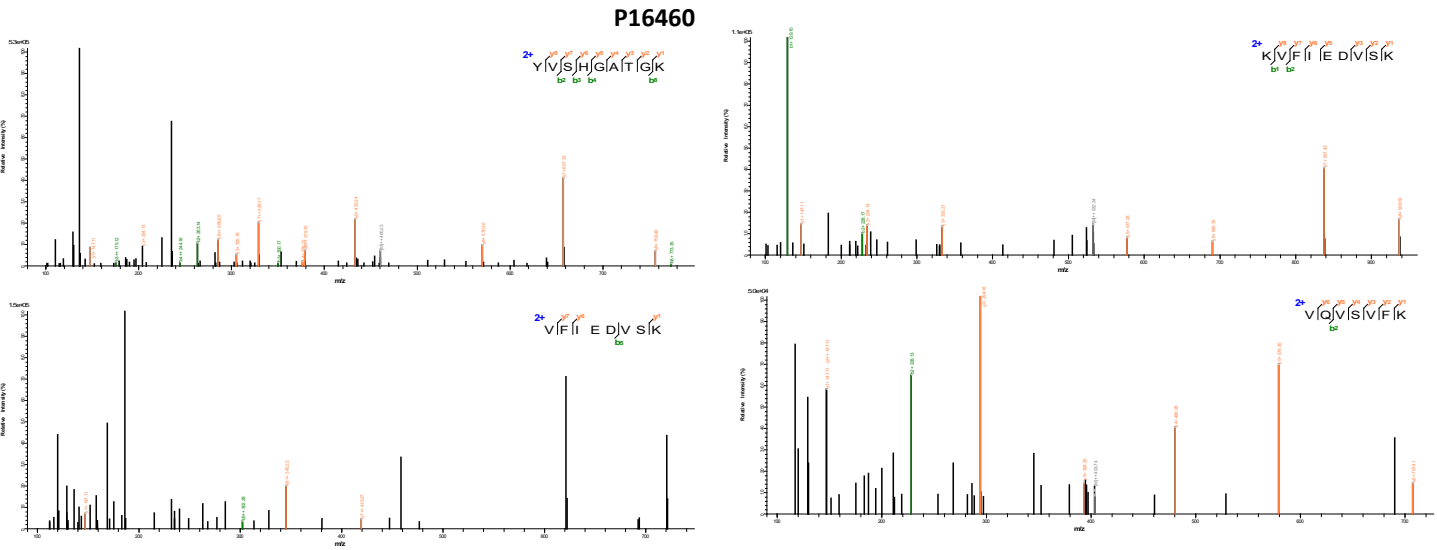

Figure S7 Secondary Mass Spectrometry of ASS1 (Protein ID: P16460).

a

Protein ID:	NP_031520.1
Defintion:	argininosuccinate synthase [Mus musculus]
Length:	412 aa

```
  1 MSSKGSVVLA YSGGLDTSCI LVWLKEQGYD VIAYLANIGQ KEDFEEARKK
 51 ALKLGAKKVF IEDVSKEFVE EFIWPAVQSS ALYEDRYLLG TSLARPCIAR
101 RQVEIAQREG AKYVSHGATG KGNDQVRFEL TCYSLAPQIK VIAPWRMPEF
151 YNRFKGRNDL MEYAKQHGIP IPVTPKSPWS MDENLMHISY EAGILENPKN
201 QAPPGLYTKT QDPAKAPNSP DVLEIEFKKG VPVKVTNIKD GTTRTTSLEL
251 FMYLNEVAGK HGVGRIDIVE NRFIGMKSRG IYETPAGTIL YHAHLDIEAF
301 TMDREVRKIK QGLGLKFAEL VYTGFWHSPE CEFVRHCIQK SQERVEGKVQ
351 VSVFKGQVYI LGRESPLSLY NEELVSMNVQ GDYEPIDATG FININSLRLK
401 EYHRLQSKVT AK
```

Motifs with high probability
Motifs with low probability
Overlapping Motifs

No.	Pos.	Group	Score	No.	Pos.	Group	Score
1	K310	REVRK I**K**QG LGLKF	0.77	6	K260	LNEVA G**K**HG VGRID	0.5
2	K239	VKVTN I**K**DG TTRTT	0.77	7	K176	PIPVT P**K**SP WSMDE	0.5
3	K53	ARKKA L**K**LG AKKVF	0.73	8	K41	LANIG Q**K**ED FEEAR	0.5
4	K215	KTQDP A**K**AP NSPDV	0.69	9	K58	LKLGA K**K**VF IEDVS	0.13
5	K228	VLEIE F**K**KG VPVKV	0.68				

b

Results for putatifs SUMO site								
Position K	Sequence	Best PS	Consensus direct			Consensus Inverted		
			Type	PSd	DB Hit	Type	PSi	DB Hit
K53	DFEEARKKALKLGAKKVFIED	None	None	None	1	None	None	1
K140	LTCYSLAPQIKVIAPWRMPEF	None	None	None		None	None	1
K228	NSPDVLEIEFKKGVPVKVTNI	Low	None	None	1	None	Low	1
K277	DIVENRFIGMKSRGIYETPAG	None	None	None		None	None	1
K308	EAFTMDREVRKIKQGLGLKFA	None	None	None	1	None	None	
K310	FTMDREVRKIKQGLGLKFAEL	None	None	None		None	None	5
K348	IQKSQERVEGKVQVSVFKGQV	High	None	None		Strong consensus inv	High	
K400	GFININSLRLKEYHRLQSKVT	None	None	None		None	None	3

c

d

Score	Expect	Method	Identities	Positives	Gaps
838 bits(2165)	0.0	Compositional matrix adjust.	399/412(97%)	407/412(98%)	0/412(0%)

```
Query  1    MSSKGSVVLAYSGGLDTSCILVWLKEQGYDVIAYLANIGQKEDFEEARKKALKLGAKKVF  60
            MSSKGSVVLAYSGGLDTSCILVWLKEQGYDVIAYLANIGQKEDFEEARKKALKLGAKKVF
Sbjct  1    MSSKGSVVLAYSGGLDTSCILVWLKEQGYDVIAYLANIGQKEDFEEARKKALKLGAKKVF  60

Query  61   IEDVSKEFVEEFIWPAVQSSALYEDRYLLGTSLARPCIARRQVEIAQREGAKYVSHGATG  120
            IEDVS+EFVEEFIWPA+QSSALYEDRYLLGTSLARPCIAR+QVEIAQREGAKYVSHGATG
Sbjct  61   IEDVSREFVEEFIWPAIQSSALYEDRYLLGTSLARPCIARKQVEIAQREGAKYVSHGATG  120

Query  121  KGNDQVRFELTCYSLAPQIKVIAPWRMPEFYNRFKGRNDLMEYAKQHGIPIPVTPKSPWS  180
            KGNDQVRFEL+CYSLAPQIKVIAPWRMPEFYNRFKGRNDLMEYAKQHGIPIPVTPK+PWS
Sbjct  121  KGNDQVRFELSCYSLAPQIKVIAPWRMPEFYNRFKGRNDLMEYAKQHGIPIPVTPKNPWS  180

Query  181  MDENLMHISYEAGILENPKNQAPPGLYTKTQDPAKAPNSPDVLEIEFKKGVPVKVTNIKD  240
            MDENLMHISYEAGILENPKNQAPPGLYTKTQDPAKAPN+PD+LEIEFKKGVPVKVTN+KD
Sbjct  181  MDENLMHISYEAGILENPKNQAPPGLYTKTQDPAKAPNTPDILEIEFKKGVPVKVTNVKD  240

Query  241  GTTRTTSLELFMYLNEVAGKHGVGRIDIVENRFIGMKSRGIYETPAGTILYHAHLDIEAF  300
            GTT  TSLELFMYLNEVAGKHGVGRIDIVENRFIGMKSRGIYETPAGTILYHAHLDIEAF
Sbjct  241  GTTHQTSLELFMYLNEVAGKHGVGRIDIVENRFIGMKSRGIYETPAGTILYHAHLDIEAF  300

Query  301  TMDREVRKIKQGLGLKFAELVYTGFWHSPECEFVRHCIQKSQERVEGKVQVSVFKGQVYI  360
            TMDREVRKIKQGLGLKFAELVYTGFWHSPECEFVRHCI KSQERVEGKVQVSV KGQVYI
Sbjct  301  TMDREVRKIKQGLGLKFAELVYTGFWHSPECEFVRHCIAKSQERVEGKVQVSVLKGQVYI  360

Query  361  LGRESPLSLYNEELVSMNVQGDYEPIDATGFININSLRLKEYHRLQSKVTAK  412
            LGRESPLSLYNEELVSMNVQGDYEP DATGFININSLRLKEYHRLQSKVTAK
Sbjct  361  LGRESPLSLYNEELVSMNVQGDYEPTDATGFININSLRLKEYHRLQSKVTAK  412
```

Figure S8 Computational prediction and cross-species conservation of ASS1 SUMOylation sites (a-c) In silico prediction of SUMO2/3 conjugation sites on ASS1 using three independent algorithms: (a) SUMOplot (Abcepta), (b) JASSA, and (c) GPS-SUMO. (d) Sequence alignment of mouse (top) and human (bottom) ASS1 showing evolutionary conservation of 19 experimentally reported SUMOylation sites (K58, K101, K112, K121, K155, K165, K176, K199, K209, K215, K228, K234, K239, K260, K310, K340, K355, K400, K408). Red asterisks denote validated sites from literature.

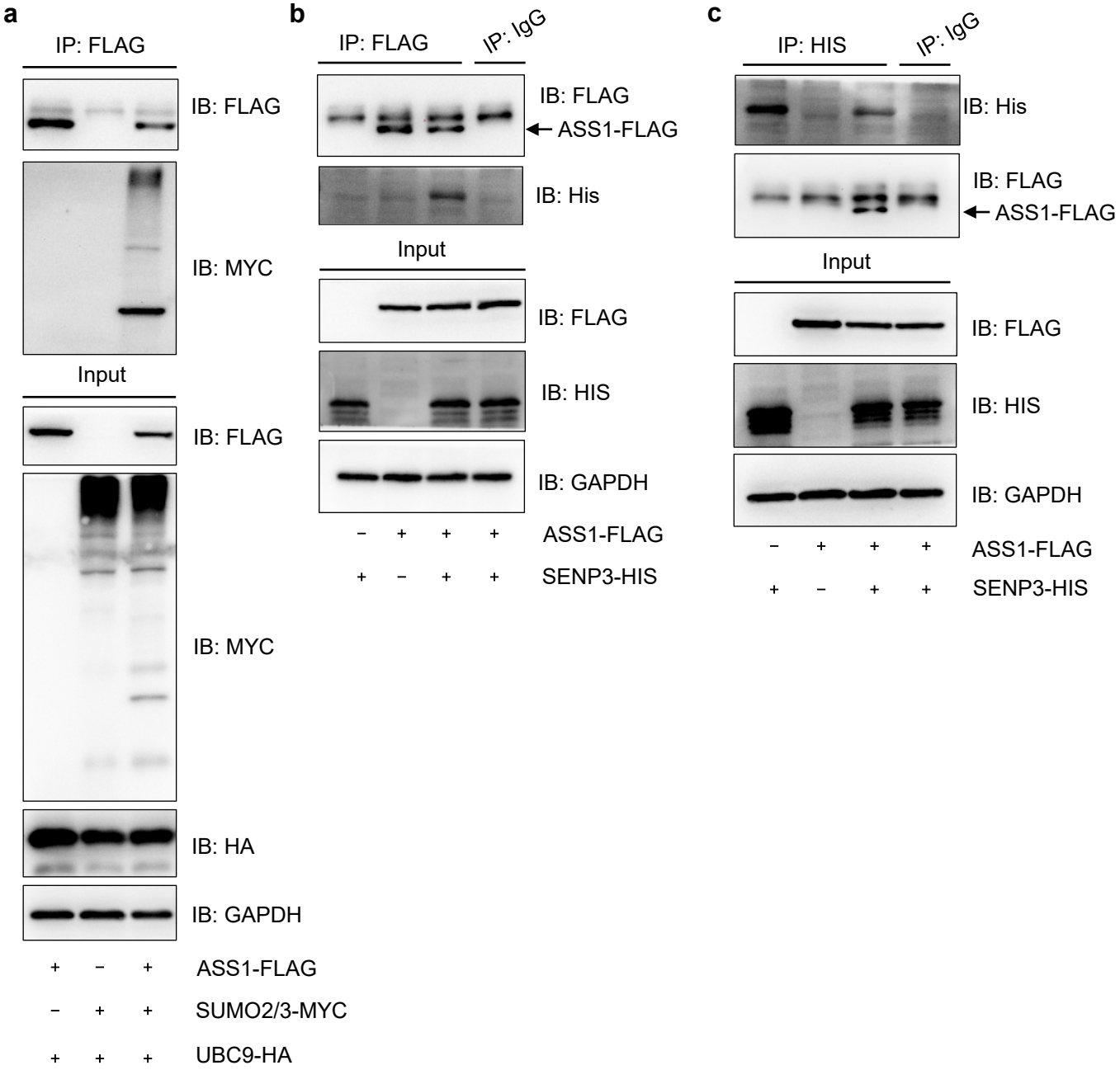

Figure S9 Exogenous interactions between ASS1, SUMO2/3, and SENP3. (a) Co-immunoprecipitation assay demonstrating interaction between FLAG-ASS1 and MYC-SUMO2/3 in HEK293T cells co-transfected with HA-UBC9 (essential E2 conjugating enzyme for SUMOylation). (b-c) Interaction studies between FLAG-ASS1 and HIS-SENP3 in transfected HEK293T cells. All experiments were performed in biological triplicates.

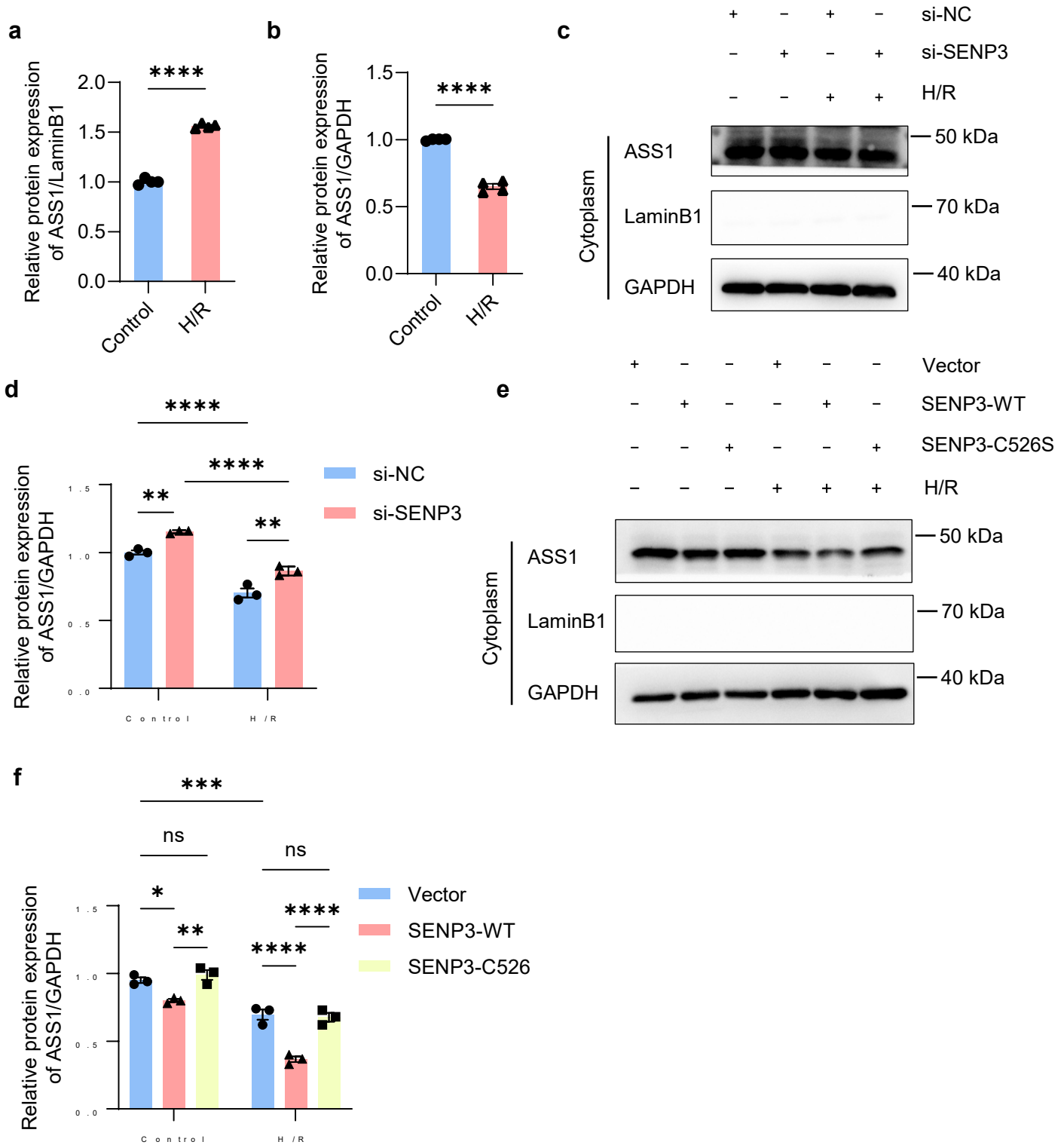

Figure S10 Subcellular fractionation analysis of ASS1 in TCMK1 cells. (a-b) Quantitative analysis of nuclear and cytoplasmic ASS1 distribution. (c-d) Cytoplasmic ASS1 levels under H/R with /without SENP3 knockdown. (e-f) Cytoplasmic ASS1 levels H/R with /without SENP3 catalytic activity. Data represent mean ± SEM (n=3 biological replicates); ns, not significant; **p<0.01, ***p<0.001, ****p<0.0001.

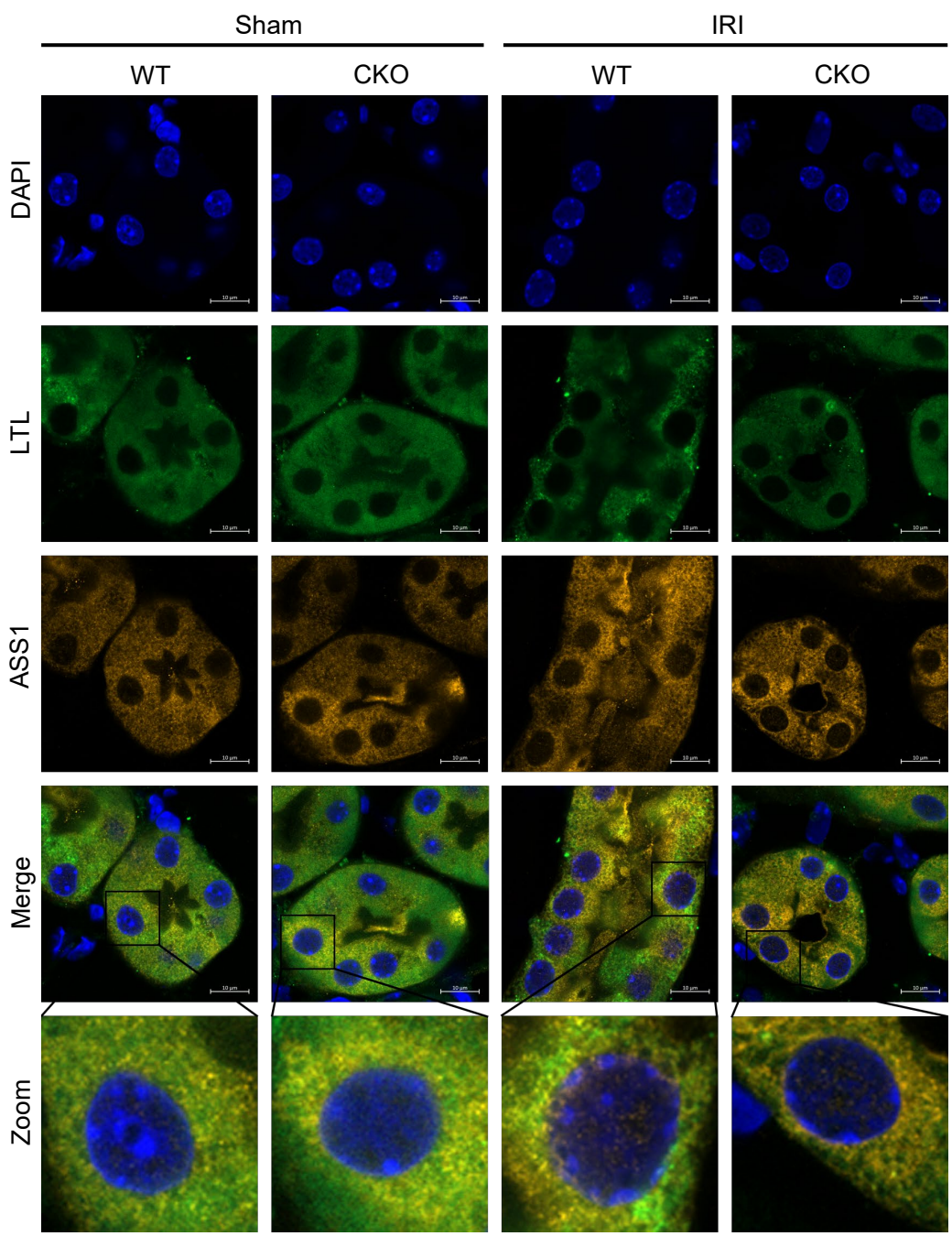

Figure S11 The ASS1 was accumulated in nuclear after IRI in renal tubular cells. Scale bar, 10μm.

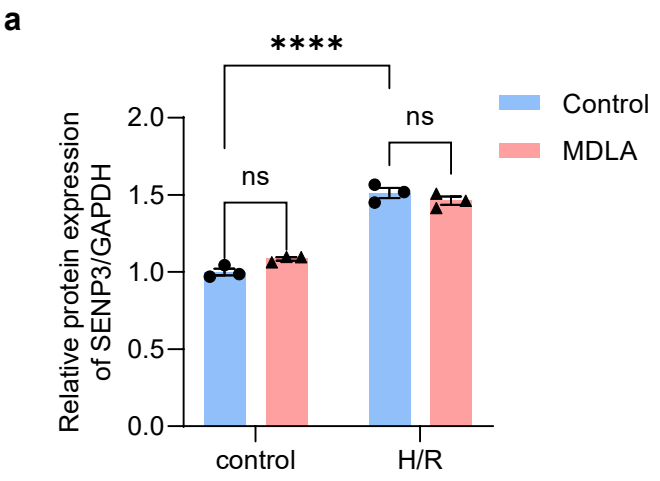

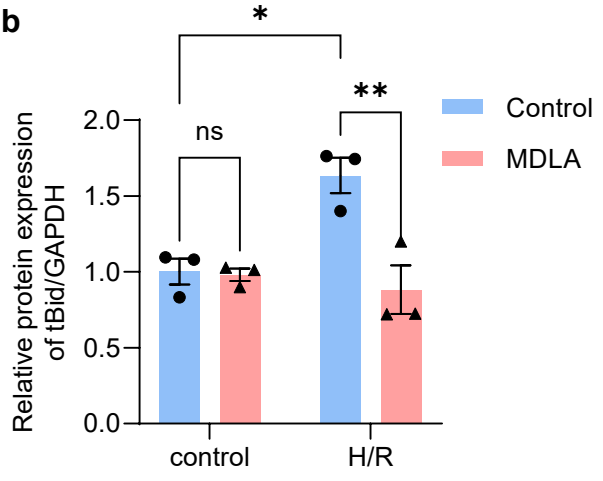

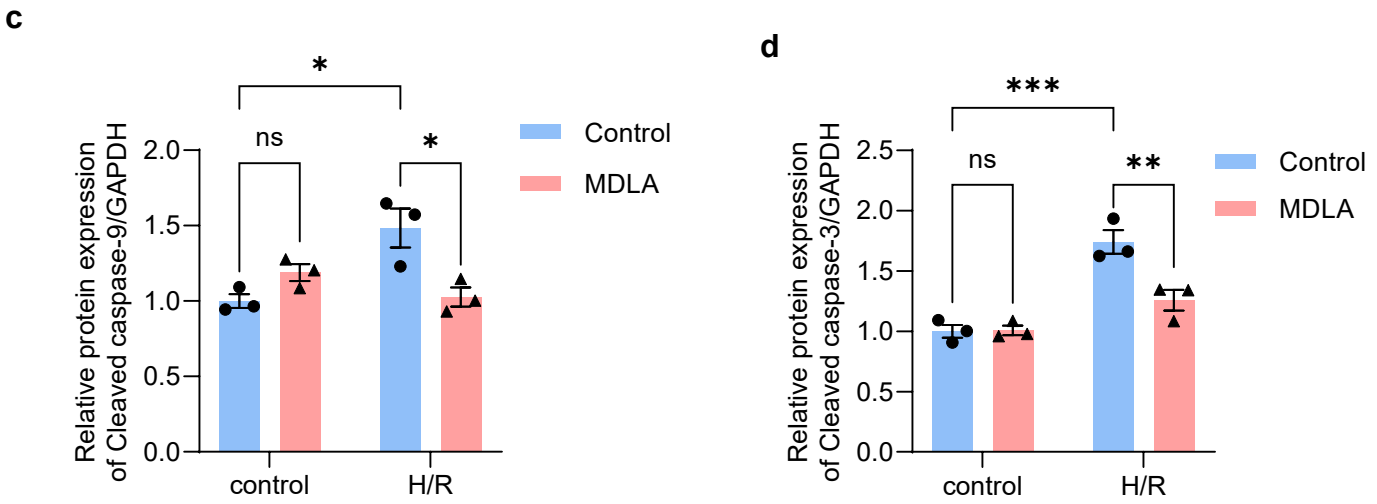

Figure S12 (a) MDLA not affected SENP3 expression. (b-d) ASS1 Inhibitor MDLA reduced cleavage of CASPASE-9/3 and PARP1 in H/R-treated TCMK1 cells. Data: mean ±SEM (n=3). ns, no significance. *p<0.05, **p<0.01, ***p<0.001.

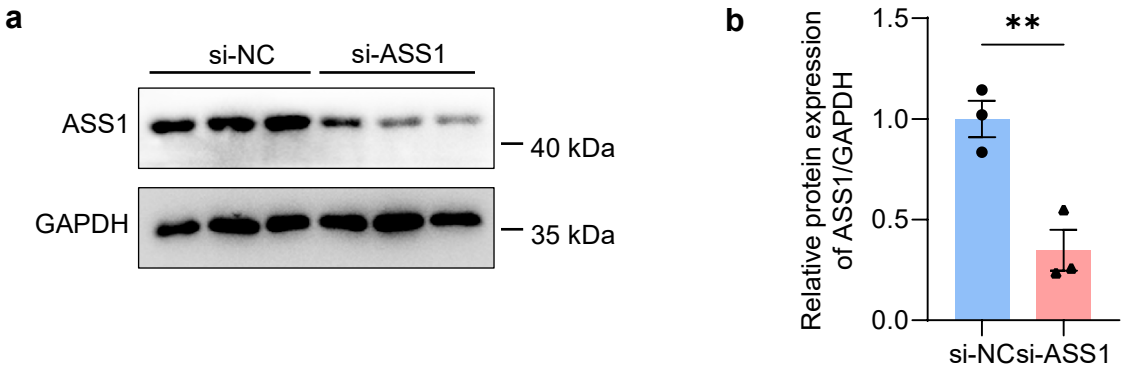

Figure S13 Efficiency of ASS1 knockdown in TCMK1 cells. (a-b) Western blot analysis and quantification showing significant reduction of ASS1 protein levels in TCMK1 cells transfected with ASS1-targeting siRNA (si-SENP3) compared to negative control siRNA (si-NC). Data represent mean ± SEM (n=3). **p < 0.01.

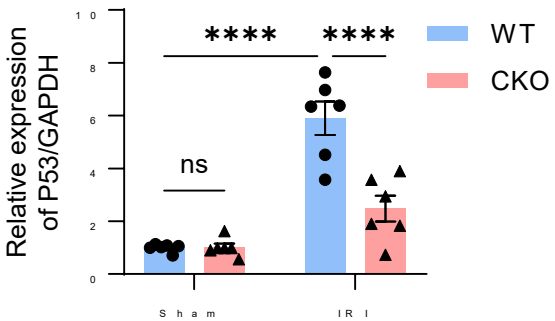

Figure S14 SENP3 deficiency reduces renal p53 expression following IRI. Data: mean ± SEM (n=6); ****p<0.0001, ns = not significant.

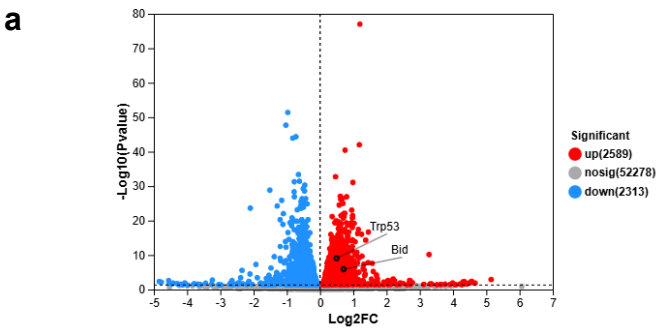

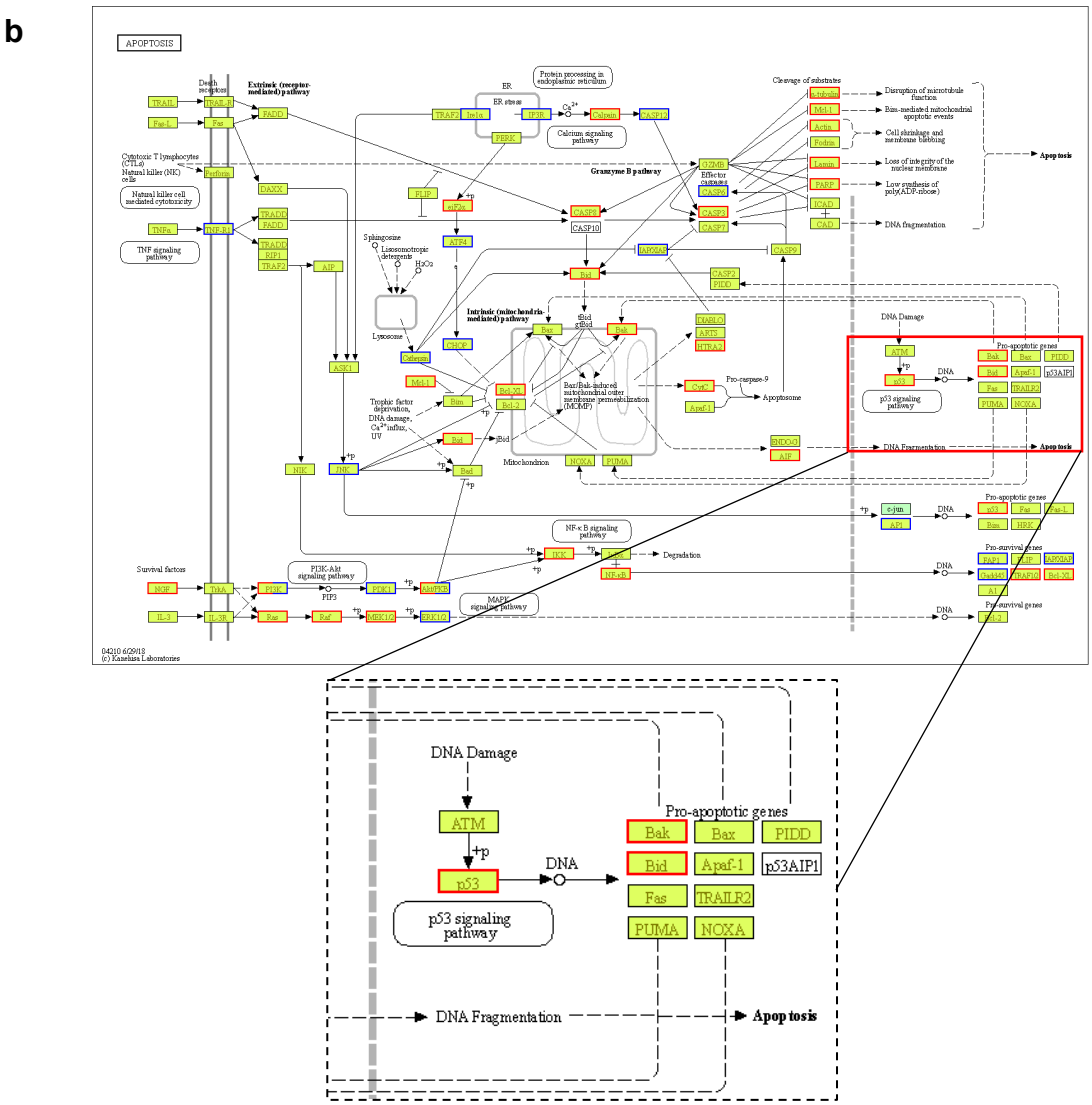

Figure S15 Hypoxia/reoxygenation (H/R) induces Trp53-mediated transcriptional activation of Bid (a) Volcano plot showing differentially expressed genes in TCMK1 mouse renal epithelial cells following H/R treatment (vs. normoxic controls). RNA-seq analysis was performed using Mus musculus reference genome (GRCm39). Differential expression was determined by DESeq2 ($p<0.05$, $n=3$). (b) KEGG pathway enrichment analysis demonstrating significant activation of apoptosis-related genes, including Bid.

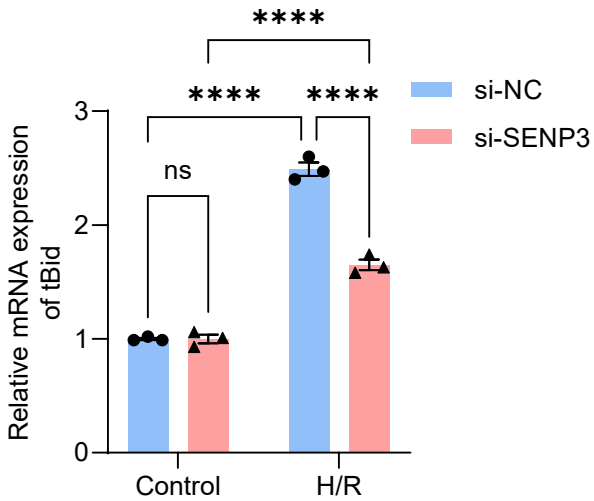

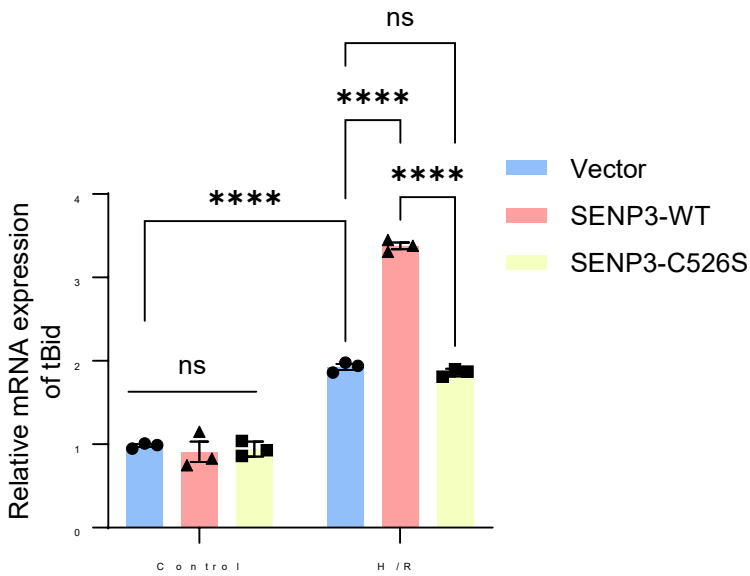

Figure S16 RT-qPCR analysis demonstrating SENP3 deSUMOylation-dependent regulation of Bid expression that paralleled Trp53 transcriptional activation. Values are mean ±SEM (n=3). ns, not significance. ****p <0.0001.